LAWRENCE
LIVERMORE
NATIONAL
LABORATORY

LLNL-JRNL-758218

Molybdenum isotope composition of uranium ore concentrate by double spike MC-ICP-MS

J. M. Rolison, M. Druce

September 14, 2018

Applied Geochemistry

Disclaimer

Title: Molybdenum isotope compositions of uranium ore concentrates by double spike MC-ICP-MS

Authors: John M. Rolison[1,*], Matthew Druce[1,2], Quinn R. Shollenberger[1,3], Theresa M. Kayzar-Boggs[1,4], Rachel E. Lindvall[1], Josh Wimpenny[1]

Affiliations:

[1] Nuclear and Chemical Sciences Division, Physical and Life Sciences Directorate, Lawrence Livermore National Laboratory, 7000 East Avenue, Livermore, CA 94551, USA

[2] Department of Chemistry and Centre for Trace Element Analysis, University of Otago, P.O. Box 56, Dunedin, New Zealand

[3] Institut für Planetologie, University of Münster, Wilhelm-Klemm-Straße 10, Münster 48149, Germany

[4] Nuclear and Radiochemistry, Los Alamos National Laboratory, MS J514, Los Alamos, NM 87545, USA

* E-mail address of the corresponding author: rolison2@llnl.gov (JM Rolison)

Keywords: molybdenum isotopes, double spike, mass-dependent isotope fractionation, nuclear forensics

Abstract

The molybdenum (Mo) isotope composition of uranium ore concentrate (UOC) has been proposed as a nuclear forensic signature due to the ubiquitous presence of Mo in the nuclear fuel cycle and to the possibility that different UOC production pathways lead to characteristic Mo isotope fractionation. Furthermore, Mo forms a volatile hexafluoride which leads to the retainment of Mo in the nuclear fuel cycle through U enrichment and reactor operation processes. As a result, it is possible that the nuclear fuel cycle generates a rich array of Mo isotope signatures. The first step in interpreting Mo isotope signatures generated during the nuclear fuel cycle is to characterize the Mo isotope composition of starting materials. In this study, a suite of UOC samples were analyzed for their Mo isotope composition in order to constrain the range of Mo isotope compositions entering the front end of the nuclear fuel cycle. Analytical protocols were developed to purify Mo from a U rich matrix prior to Mo isotope analysis by double spike MC-ICP-MS. A >3‰ variation in the $^{98}Mo/^{95}Mo$ ratio was observed in the suite of UOC samples with $\delta^{98}Mo$ ranging from -1.15 to +1.96‰ relative to the NIST 3134 Mo standard reference material. The $\delta^{98}Mo$ range observed in the UOC samples is very similar to the $\delta^{98}Mo$ range observed in crustal igneous rocks and Mo-bearing minerals, suggesting that Mo isotope variability in UOC is driven by variability in the parent U ores. However, Mo isotope fractionation during UOC production is evident with one of the UOC samples being isotopically heavy relative to its parent U ore by 0.75‰, suggesting that different UOC production processes also contribute to the total Mo isotope variability observed. Overall, it is expected that the Mo isotope signatures generated during enrichment and reactor process will be clearly discernable from those generated during UOC production.

1. Introduction

Nuclear forensic science seeks to exploit signatures contained within nuclear materials found outside of regulatory control to address questions such as: Where did the material originate? What is the intended use of the material? When was the material lost from regulatory control? And ultimately, who can be held responsible if any laws were broken? Uranium ore concentrate (UOC) is produced from the mining and milling of uranium ore, and as such, represents an early product in the nuclear fuel cycle. The uranium concentration in modern UOC is typically between 60 and 80% and UOC can be composed of various chemical compounds including uranium oxide, ammonium diuranate, sodium diuranate, uranyl hydroxide, and uranyl peroxide (Kristo et al., 2016). Uranium ore concentrate, the first regulated material in the nuclear fuel cycle, is easily transported and is traded as a commodity in the global market (Kristo and Tumey, 2013). As such, diversion of UOC from the civilian power industry to weapons production is a genuine concern. Brennecka et al. (2010) suggested that natural variability in the $^{235}U/^{238}U$ and $^{234}U/^{238}U$ isotope ratios in UOC is related to the redox conditions of the depositional environment in which the parent uranium ore was deposited and can therefore be used to coarsely narrow down the possible source material of UOC. Although UOC is rich in uranium, it is generally not an exceptionally pure material and various impurities can exist at elevated concentrations. The concentrations of major and trace elements, rare earth element patterns, and the isotope compositions of certain trace elements, e.g. Sr, Nd and Pb, can provide additional information in determining the most likely source of UOC (e.g. Švedkauskaite-LeGore et al., 2008; Keegan et al., 2008; Varga et al., 2009; Krajkó et al., 2014; Varga et al., 2017), including the U ore deposit or the milling operation that produced the UOC. Ultimately, a complex suite of parameters is required to confidently constrain the origin of any nuclear material. To obtain more discriminatory power and confidence when interrogating unknown samples, it is desirable to increase the number of available signatures that can be exploited. Furthermore, signatures that are able to persist throughout the nuclear fuel cycle are of high importance.

Molybdenum (Mo) is a trace element within Earth's crust with a typical concentration of ca. 1 µg g^{-1} (Wedepohl, 1995), is often found at elevated concentrations in uranium ores, and is difficult to separate from U during the UOC production process which can lead to high Mo

concentrations in the final UOC product (IAEA, 1993). Molybdenum has seven stable isotopes that have abundances ranging from ca. 9 to 24%. Variability in the Mo isotope composition of natural materials has been investigated extensively for nearly two decades and continual improvements in analytical protocols now allow for Mo isotope ratios to be measured with a precision of 0.05‰ or less. Similar to U, Mo isotope fractionation occurs during shifts in environmental redox conditions (e.g. Arnold et al., 2004; Neubert et al., 2008) and Mo isotope ratios in UOC may therefore be useful in distinguishing different parent U ore deposit types. In addition to persisting as a trace element throughout the UOC production process, Mo forms a volatile hexafluoride (MoF_6) with a boiling point of 34 °C (Cady and Hargreaves, 1961). Thus, Mo originating from the parent uranium ore may persist through the UOC production process, into the nuclear fuel cycle beyond the uranium fluorination process, and in to the enrichment and reactor processes. It is expected that Mo isotope fractionation will occur during enrichment and neutron induced transformations will occur during reactor operation. Such isotope fractionation and transformations may result in useful nuclear forensic signatures, which emphasizes the importance of characterizing the Mo isotope composition of UOC materials before interpreting Mo isotope signatures from materials farther along in the nuclear fuel cycle.

Two previous studies have investigated Mo isotope compositions in U rich materials. Migeon et al. (2015) presented data for four UOC uranium reference materials distributed by CETAMA (France). The four samples displayed ca. 3‰ variability in the $^{98}Mo/^{95}Mo$ ratio with $\delta^{98}Mo$ ranging between -2.82 and +0.05‰ (where $\delta^{98}Mo$ is the relative difference in the $^{98}Mo/^{95}Mo$ ratio between the sample and NIST SRM-3134). Migeon et al. (2018) presented a thorough leaching experiment designed to mimic industrial leaching processes used in UOC production to extract U from U bearing ores. Their leaching experiments demonstrated that under various chemical leaching conditions employing sulfuric acid and different oxidizing agents, Mo leached from granitic U ore is consistently isotopically heavy by up to ca. 1.4‰ in the $^{98}Mo/^{95}Mo$ ratio. Molybdenum isotope fractionation between leached Mo and the bulk ore Mo can be attributed to the preferential dissolution of different Mo-bearing minerals present in the bulk ore, adsorption of dissolved Mo onto particulate surfaces, and precipitation of secondary Mo minerals (Migeon et al., 2018). Thus, there is disagreement between the UOC samples analyzed by Migeon et al. (2015) that contained isotopically light Mo and the leaching experiments by Migeon et al. (2018)

that predict UOC should contain isotopically heavy Mo. A more comprehensive set of UOC samples would aid in resolving this discrepancy and would allow for better constraints to be placed on the Mo isotope compositions in UOC entering the nuclear fuel cycle.

In this study, we present Mo isotope compositions for a suite of UOC samples from multiple localities worldwide that were produced using various production methods. The sample suite also includes one paired set of UOC product and its parent U ore. The results provide improved constraints on the range of Mo isotope compositions in UOC and further demonstrate the potential of Mo isotopes as a nuclear forensic signature.

2. Materials and Methods

All mineral acids (HNO_3, HCl, HF) and hydrogen peroxide (H_2O_2) used for digestions and purification chemistry were ultra-high purity grade (Baseline®, Seastar Chemicals Inc™). All water used for rinsing and making dilutions was 18.2 MΩ-cm supplied by a Milli-Q® water purification system (Millipore-Sigma). Prior to use, all fluorinated ethylene propylene (FEP) and perfluoroalkoxy (PFA) bottles and vials were cleaned by sequentially soaking in warm 1% Basic-H® detergent (Shaklee, Inc.) for ~24 h followed by 8 M HNO_3 at 120°C for at least 48 h. Savillex PFA vials were further refluxed on a hot plate at 120°C with 6 M HCl + 1 M HF for at least 24 h. Labware was rinsed with copious amounts of Milli-Q® water after each cleaning step.

2.1 Double spike preparation

The double spike technique is a robust and efficient method for determining high-precision isotope ratios. Mass-dependent isotope fractionation that occurs during sample processing as a result of incomplete yield from purification chemistry and mass fractionation within mass spectrometers can be accurately corrected through the use of a double spike, provided that the double spike is added to the sample prior to any processing. Furthermore, the double spike technique can also handle low amounts of matrix elements remaining in the sample after

purification (e.g. Creech et al., 2017) while maintaining high accuracy and precision, and allows for the determination of the elemental concentration via isotope dilution simultaneously.

The application of the double spike technique is limited to elements that have four or more isotopes. Molybdenum has seven stable isotopes and thus, multiple double spike designs are possible. The most common Mo double spike applied in the isotope geochemistry community is a ^{97}Mo-^{100}Mo double spike (e.g. Sibert et al., 2001; McManus et al., 2002; Nägler et al., 2005; Archer and Vance, 2008; Dahl et al., 2010; Skierszkan et al., 2015; Migeon et al., 2015). Sibert et al. (2001) initially decided on a ^{97}Mo-^{100}Mo double spike because ^{97}Mo and ^{100}Mo have relatively low natural abundance, do not suffer from significant elemental isobaric interferences (aside from ^{100}Ru which is generally negligible), and highly enriched single spikes of ^{97}Mo and ^{100}Mo were available from Oak Ridge National Laboratory (ORNL). Moreover, the choice of ^{95}Mo, ^{97}Mo, ^{98}Mo, and ^{100}Mo as the four isotopes to be used in the double spike inversion avoids Mo isotopes that suffer from Zr isobaric interferences which can be more difficult to prevent. Error modelling work by Rudge et al. (2009) predicts that the combination of a ^{97}Mo-^{100}Mo double spike and a ^{95}Mo-^{97}Mo-^{98}Mo-^{100}Mo inversion results in an error of ca. 32 ppm amu^{-1} in the final corrected isotope ratios of the sample.

Highly enriched single spikes of ^{97}Mo (94.2%) and ^{100}Mo (99.4%) in the form of metal powders were purchased from ORNL (Table 1). The two spikes were separately weighed and transferred to Savillex vials before dissolution in 8 M HNO_3. The spikes were subsequently transferred to 250 mL FEP bottles and diluted to concentrations of ~10 ppm. The ^{97}Mo-^{100}Mo double spike was prepared in a 1 L FEP bottle by mixing aliquots of the two single spikes while aiming for proportions of ca. 37% ^{97}Mo and 63% ^{100}Mo, which is the ^{97}Mo-^{100}Mo double spike composition recommended by Rudge et al. (2009). The ^{97}Mo-^{100}Mo mixture was refluxed before being diluted to a concentration of ~500 ppb.

The double spike was calibrated against NIST 3134 Mo standard reference material using the Mo isotope composition of NIST 3134 reported by Mayer and Wieser (2014) (Table 1). The accuracy of the double spike calibration was tested by analyzing open ocean seawater samples for their Mo isotope compositions. Open ocean seawater is very homogenous with respect to Mo

isotope composition (Goldberg et al, 2013) and is therefore an ideal secondary isotope standard since it is easily obtainable by the international community. Open ocean seawater was obtained from the GEOTRACES program (SAFe D1 #590; geotraces.org) and from the National Research Council Canada (NASS-7). Additionally, United States Geological Survey (USGS) reference material BCR-2, a basalt from the Columbia River, Oregon, USA, and a Mo ICP standard (Inorganic Ventures™, USA) were utilized for quality control.

Table 1
Isotope compositions of single spikes, double spike, and NIST SRM-3134.

	^{92}Mo (%)	^{94}Mo (%)	^{95}Mo (%)	^{96}Mo (%)	^{97}Mo (%)	^{98}Mo (%)	^{100}Mo (%)
^{97}Mo single spike[a]	0.22	0.19	0.47	1.25	94.19	3.37	0.31
^{100}Mo single spike[a]	0.01	0.02	0.04	0.05	0.04	0.46	99.40
^{97}Mo-^{100}Mo double spike	0.10	0.08	0.20	0.50	35.74	1.56	61.81
NIST SRM-3134[b]	14.65	9.19	15.87	16.67	9.58	24.29	9.74

[a] Oak Ridge National Laboratory certificate values
[b] Values reported by Mayer and Wieser (2014)

2.2 Sample description and chemical processing

Samples of UOC from different geographic locations were obtained from the UOC sample library at Lawrence Livermore National Laboratory. Additionally, three samples from the South African AngloGold-Ashanti South Uranium Plant representing a paired U ore with two UOC products were obtained from the International Atomic Energy Agency (IAEA). These three samples consist of (1) the incoming parent U ore, (2) a sample of ammonium diuranate (ADU) that is the final product of uranium processing plant, and (3) a U_3O_8 sample produced by calcination of the ADU at 490°C at a separate processing facility (Marks et al., 2015). Importantly, these three samples were collected at the same time along the uranium processing circuit which should ensure the Mo contained within in the three samples has the same origin. All samples were stored as powders in polypropylene bottles until they were subsampled.

Two batches of samples were processed separately and in different ways. For the first batch of samples, ~100 mg of powdered sample was weighed into 15 mL Savillex perfluoroalkoxy (PFA) vials and dissolved in 3 mL of 10.5 M HCl + 50 μL conc. HNO_3. The vials were refluxed on a

hotplate at 120°C for 24 h. This digestion procedure resulted in clear solutions that were ready for an initial separation of Mo from the U-rich matrix via anion exchange chemistry. The samples were loaded on to Bio-Rad Poly-Prep® chromatography columns containing 2 mL of Bio-Rad AG® 1-X8 (100-200 mesh) anion exchange resin. The resin was then rinsed with an additional 5 mL of 10.5 M HCl. The initial load and rinse solutions were collected and retained for analysis of rare earth elements. Uranium was eluted with 12 mL of 0.5 M HCl + 0.5 M HF. Finally, molybdenum was eluted with 15 mL of 1 M HCl. Since Mo isotope fractionation can occur during anion exchange chemistry (e.g. Sibert et al., 2001), four of the UOC samples processed in the first batch were replicated in the second batch of samples which were double spiked prior to anion exchange chemistry.

For the second batch of samples, ~250 mg of powdered sample was transferred in to PFA microwave digestion vials, 10 mL of 1:3 HF:HNO_3 was added, and the vials were placed in a Milestone ETHOS microwave digestion system. After microwave digestion, the samples were transferred to 30 mL Savillex PFA vials and evaporated to dryness on a hotplate at 120°C. The dried samples were then dissolved in ~15 mL of 4 M HNO_3 + 0.005 M HF.

Both batches of samples were processed identically from this point forward and the open ocean seawater samples and dissolutions of USGS BCR-2 were processed alongside the samples for quality control. The concentration of Mo in the eluted fraction from the first batch of samples and in the primary dissolution solutions from the second batch of samples was determined via ICP-MS (Element 2™, Thermo Scientific) using a multi-element external standard calibration. Aliquots of each sample containing ~250 ng Mo were transferred to clean 15 mL Savillex PFA vials. A ^{97}Mo-^{100}Mo double spike was added to each sample aiming for a spike/sample ratio of ~1. The sample-spike mixtures were refluxed on a hotplate at 120°C for ~24 to promote isotopic equilibrium between the sample and spike. The samples were evaporated to dryness, dissolved in 1 mL of 6 M HCl and loaded onto Bio-Rad Poly-Prep® columns containing 1 mL Bio-Rad AG® 1-X8 (100-200 mesh) anion exchange resin. The columns were successively rinsed with 8 mL of 6 M HCl to elute most matrix elements, 8 mL of 0.5 M HCl + 0.5 M HF to elute U together with Fe, and 8 mL of 1 M HCl to elute Mo (Fig. 1). Fig. 1 also illustrates the multi-element capability of the purification method with purified fractions of Zn and Cd eluted in 2 M HNO_3 + 0.1 M

HBr and 2 M HNO_3, respectively, after the Mo fraction is eluted. The purified Mo fractions were evaporated to dryness and residual organics derived from the resin were destroyed by refluxing in concentrated HNO_3 + H_2O_2 (1:1). The samples were dried down and the anion exchange purification procedure was repeated a second time. After completion of the purification chemistry, samples were dissolved in the analysis solution (0.56 M HNO_3 + 0.005 M HF) in preparation for Mo isotope ratio analysis via multiple collector inductively coupled plasma mass spectrometry (MC-ICP-MS). The total procedural blank determined by isotope dilution MC-ICP-MS averaged ~1.2 ng (n = 3), which is <0.5% of the sample and is thus inconsequential.

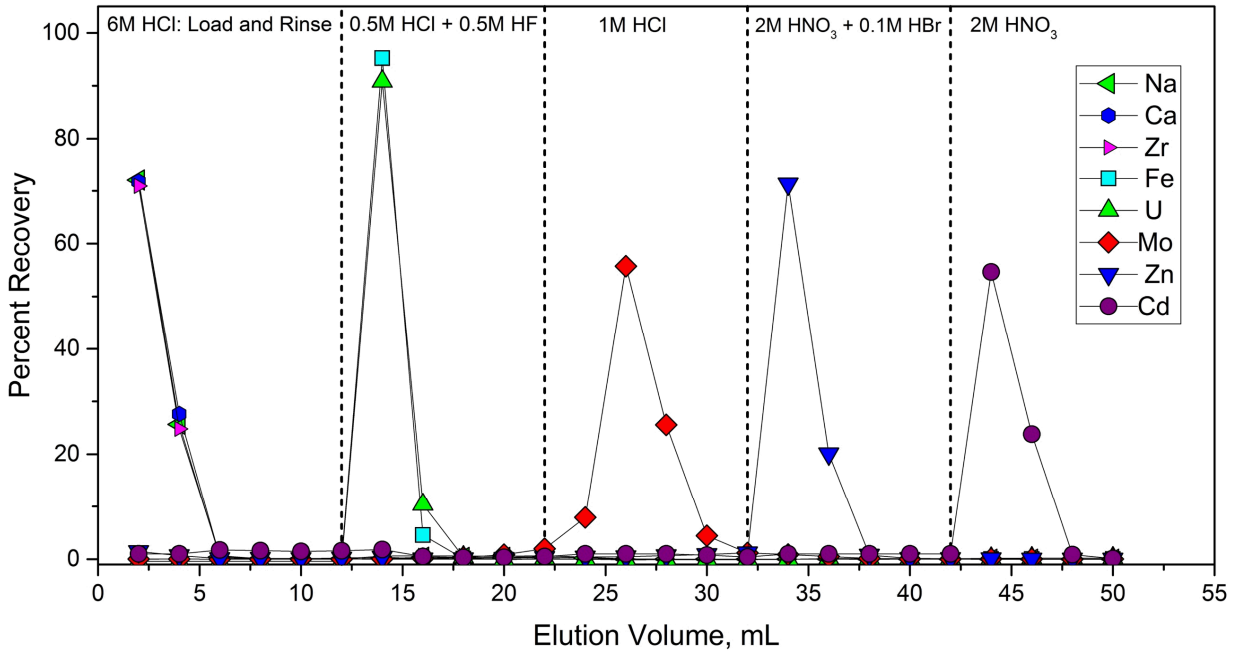

Fig. 1. Elution profile of a sample of BCR-2 using 1 mL of anion exchange resin.

2.3 Mass spectrometry

All Mo isotope ratio analyses were made using the *Nu Instruments* Nu Plasma II MC-ICP-MS at LLNL. Molybdenum isotope analyses were made in low mass resolution mode. A Cetac 100 µL min^{-1} self-aspirating nebulizer in combination with a Cetac Aridus II™ desolvating system were used to introduce the sample into the plasma. The Nu Plasma II is equipped with an array of 16 fixed position Faraday detectors which allows for the simultaneous detection of all Mo isotopes and interference free isotopes of neighboring elements Zr and Ru which are used as interference

monitors on the Mo isotope masses (Table 2). All Faraday cups were connected to 10^{11} Ω resistors. A 60 s on-peak baseline measurement of the 0.56 M HNO_3 + 0.005 M HF analysis solution was performed between each Mo isotope analysis. The measured baseline was subtracted from the subsequent Mo isotope analysis which consisted of a static measurement of 30 cycles with an 8 s integration time each. Samples and standards were analyzed at a Mo concentration of ~50 ppb which resulted in a total ion beam intensity of ~20 V and a total consumption of ~25 ng Mo per analysis. All sample analyses were bracketed with the NIST 3134 Mo standard reference material, which was double spiked similarly to the samples.

Table 2
Collector configuration of the Nu Plasma II MC-ICP-MS for Mo isotope ratio analyses and natural isotope abundances.

Collector	H5	H4	H3	H2	H1	Ax	L1	L2	L3	L4	L5
Mo Isotopes monitored		^{100}Mo		^{98}Mo	^{97}Mo	^{96}Mo	^{95}Mo	^{94}Mo		^{92}Mo	
Abundances (%)		(9.75)		(24.3)	(9.58)	(16.7)	(15.9)	(9.19)		(14.7)	
Ru Isotopes monitored	^{101}Ru	^{100}Ru	^{99}Ru	^{98}Ru		^{96}Ru					
Abundances (%)	(17.1)	(12.6)	(12.8)	(1.87)		(5.54)					
Zr Isotopes monitored						^{96}Zr		^{94}Zr		^{92}Zr	^{90}Zr
Abundances (%)						(2.8)		(17.4)		(17.2)	(51.5)

The measured Mo isotope ratios in both standards and samples were corrected for isobaric interferences from Ru using the monitored $^{99}Ru^{+}$ ion beam, instrumental mass fractionation and the contribution of the double spike at the cycle level using an off-line double spike data reduction procedure following Sibert et al. (2001). The double spike correction assumes that all mass-dependent fractionations follow the exponential mass fractionation law. The four Mo isotopes used in the double spike inversion were ^{95}Mo, ^{97}Mo, ^{98}Mo, and ^{100}Mo, thereby eliminating any potential issues arising from Zr corrections. The internal uncertainty (2 s.e.) for each double spike corrected Mo isotope ratio analysis is typically ~0.05‰ and accounts for the combined uncertainty from the analysis of the sample and the two NIST 3134 bracketing standards. In accordance with recommended reporting guidelines (Goldberg et al., 2013), the final Mo isotope ratios are reported as the permil relative difference in the ^{98}Mo/^{95}Mo ratio between the sample and the average of the two NIST 3134 bracketing standards:

$$\delta^{98}\mathrm{Mo} = \left[\frac{(^{98}\mathrm{Mo}/^{95}\mathrm{Mo})_{\mathrm{sample}}}{(^{98}\mathrm{Mo}/^{95}\mathrm{Mo})_{\mathrm{NIST-3134}}} - 1\right] \times 10^{3}$$

3. Results

3.1 Accuracy and precision of Mo isotope measurements

The performance of the Mo isotope measurements was assessed by regularly analyzing a commercial Mo ICP standard (Inorganic Ventures, USA) as a secondary isotope standard. This material was not processed through any chemical purification procedure and was simply mixed with the Mo double spike in appropriate proportions, dried down, and dissolved in the MC-ICP-MS analysis solution. The repeated analysis of the Mo ICP standard yielded a δ^{98}Mo of -0.41 ± 0.05‰ (2 s.d., n = 17) (Fig. 2) which demonstrates the long-term precision of Mo isotope measurements achievable using the double spike technique employed in this study. Furthermore, the isotopic difference between the Mo ICP standard and NIST 3134 is similar to the range of the isotope compositions of -0.37 to -0.16‰ observed for multiple Mo ICP standards utilized internationally as in-house standards (e.g. Goldberg et al., 2013).

The two open ocean seawater samples utilized in this study (i.e. SAFe D1 and NASS-7) yielded identical Mo isotope compositions with a mean δ^{98}Mo of +2.10 ± 0.09‰ (2 s.d., n = 8) (Fig. 2). Multiple aliquots of each seawater standard were processed alongside the samples (Table 3). Goldberg et al. (2013) reported a mean δ^{98}Mo of +2.09 ± 0.10‰ for a compilation of 26 different seawater samples that were analyzed in various laboratories internationally. Seawater results from this study are in excellent agreement with the consensus value reported by Goldberg et al. (2013), which demonstrates that the double spike procedure results in accurate Mo isotope ratios. In addition to the seawater samples, a single dissolution of BCR-2 was split into three separate samples, which were double spiked and processed through anion exchange chemistry individually. Each purified aliquot contained enough Mo for three MC-ICP-MS analyses. The triplicate analyses of the three BCR-2 aliquots yielded a mean δ^{98}Mo of +0.01 ± 0.03‰ (2 s.d., n = 9). Although BCR-2 has not been widely analyzed for its Mo isotope composition, our data agree with the recent studies by Skierszkan et al. (2015) and Liang et al. (2017) who report

312 δ^{98}Mo of -0.04 ± 0.10‰ (2 s.d., *n* = 3) and -0.03 ± 0.04‰ (2 s.d., *n* = 3), respectively, for BCR-
313 2. Both the open ocean seawater samples and BCR-2 samples analyzed in this study show good
314 reproducibility between multiple replicates processed through the purification chemistry,
315 indicating the methods employed result in accurate and precise Mo isotope compositions.
316

Table 3

Molybdenum isotope composition of reference materials.

Reference Material	δ^{98}Mo, ‰	2 s.e.[a]
Seawater		
SAFe D1	+2.19	0.04
SAFe D1	+2.10	0.04
NASS-7	+2.13	0.04
NASS-7	+2.07	0.05
NASS-7	+2.10	0.06
NASS-7	+2.04	0.05
NASS-7	+2.07	0.05
NASS-7	+2.11	0.04
average and 2 s.d.	*+2.10*	*0.09*
USGS basalt		
BCR-2 #1	+0.02	0.05
BCR-2 #1	+0.01	0.05
BCR-2 #1	+0.02	0.05
BCR-2 #2	+0.00	0.04
BCR-2 #2	+0.02	0.05
BCR-2 #2	-0.01	0.05
BCR-2 #3	-0.02	0.05
BCR-2 #3	-0.00	0.05
BCR-2 #3	+0.02	0.05
average and 2 s.d.	*+0.01*	*0.03*
ICP Mo standard	-0.36	0.04
ICP Mo standard	-0.40	0.04
ICP Mo standard	-0.37	0.04
ICP Mo standard	-0.45	0.06
ICP Mo standard	-0.45	0.04
ICP Mo standard	-0.40	0.05
ICP Mo standard	-0.44	0.04
ICP Mo standard	-0.40	0.04
ICP Mo standard	-0.43	0.04
ICP Mo standard	-0.39	0.05
ICP Mo standard	-0.44	0.05
ICP Mo standard	-0.39	0.06
ICP Mo standard	-0.40	0.04
ICP Mo standard	-0.44	0.05
ICP Mo standard	-0.40	0.05
ICP Mo standard	-0.40	0.05
ICP Mo standard	-0.39	0.05
average and 2 s.d.	*-0.41*	*0.05*

[a] Uncertainty is 2×standard error of a single mass spectrometric analysis.

317

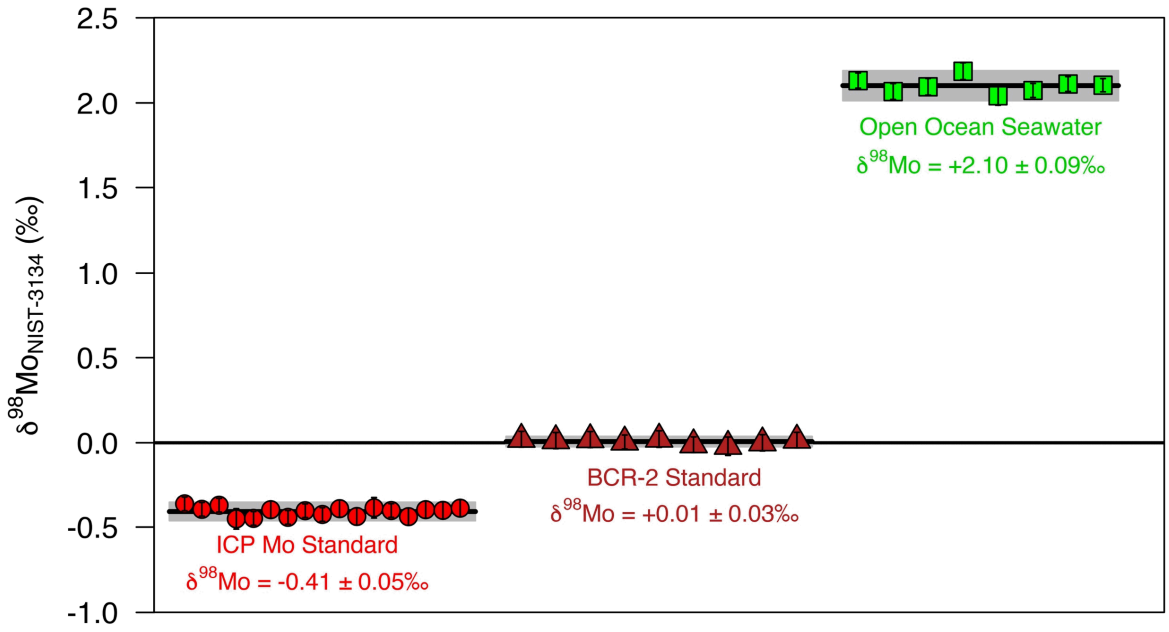

Fig. 2. Molybdenum isotope composition of reference materials. The black line and grey box represent the average and 2 s.d. uncertainty, respectively. Uncertainties shown for each data point are the internal uncertainties (2 s.e.) obtained from the mass spectrometric analysis and are generally smaller than the symbol.

3.2 Molybdenum isotope composition of uranium ore concentrates

Thirty-one samples of uranium ore concentrate (UOC) and one uranium ore were analyzed for their Mo isotope compositions. The full analytical procedure was duplicated for four of the UOC samples. The UOC samples display a δ^{98}Mo range of -1.15 to +1.96‰ (Table 4; Fig. 3). Two of the duplicated UOC samples (Canada – Stanrock and Romania – Feldioara) show excellent agreement while the other two UOC (Australian – Rum Jungle and Canada – Gunnar) show minor disagreement of ~0.10‰, which is slightly outside the stated uncertainty. Importantly, the duplicate UOC samples were processed separately in each of the two batches of samples (Table 3). Overall, the agreement between the duplicated UOC samples is considered acceptable and demonstrates that the first batch of samples is unlikely to have experienced significant fractionation during the first anion exchange column that was performed prior to the addition of the Mo double spike. The slight disagreement observed between two of the duplicated UOCs

may reflect slight heterogeneity in the samples. Moreover, the most extreme δ^{98}Mo values (i.e. Yugoslavia – Spisak-Black and USA – Federal American Partners) and all negative δ^{98}Mo values observed are in UOC samples from the second batch of samples that were double spiked prior to any purification chemistry. Thus, it is unlikely that the large variability in δ^{98}Mo observed in UOCs is an analytical artifact.

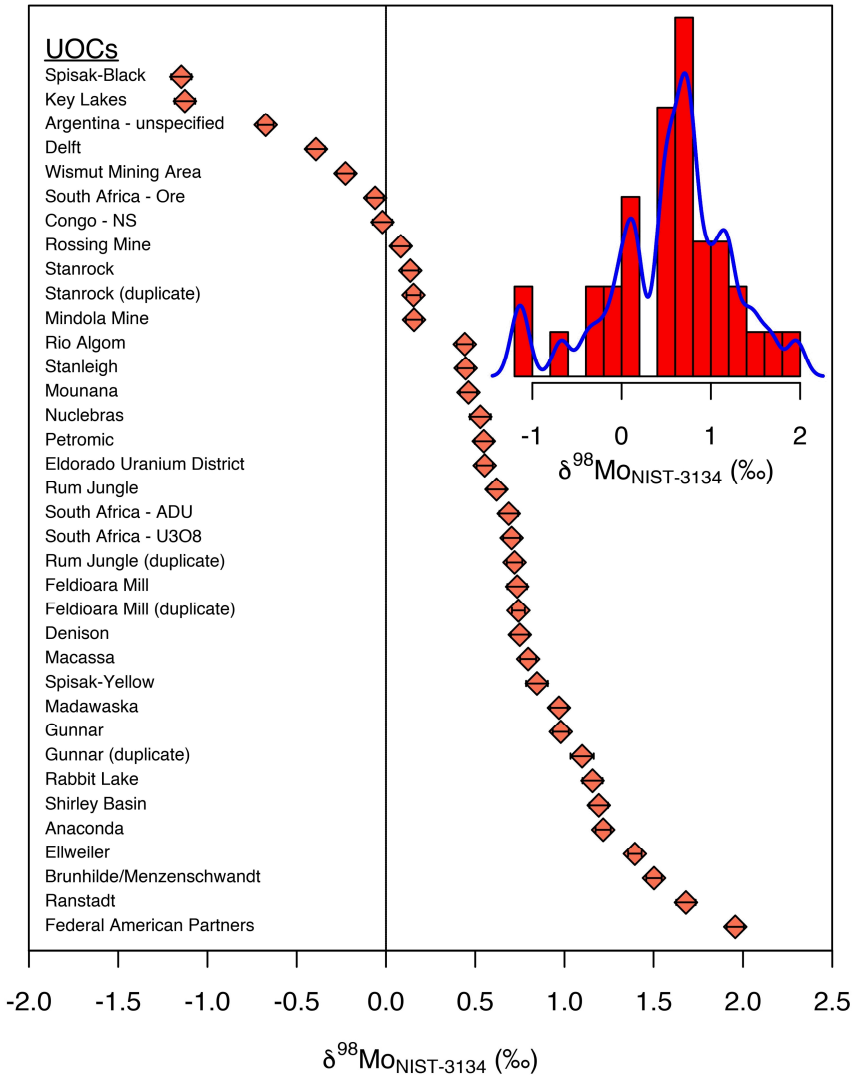

Fig. 3. Molybdenum isotope composition of uranium ore concentrate (UOC) samples from various geographic locations ordered by δ^{98}Mo. Uncertainty on the data points represents the internal uncertainty (2 s.e.) from the mass spectrometric analysis. Error bars are typically smaller the symbols. The inset is a histogram of the UOC Mo isotope compositions.

Table 4
Sample identifications, elemental concentrations, and Mo isotope compositions.

Country - Mine Name	Batch[a]	[U] g g^{-1}	[Al] µg g^{-1}	[K] µg g^{-1}	[Fe] µg g^{-1}	[Mo] µg g^{-1}	[Th] µg g^{-1}	δ^{98}Mo, ‰	2 s.e., ‰[b]
Argentina - unspecified	2	0.78	471	213	773	844	0.86	-0.67	0.04
Australia - Rum Jungle	1	0.58	4910	791	32500	36.2	8.31	+0.62	0.05
Australia - Rum Jungle (duplicate)	2	0.49	5880	879	36000	37.7	10.6	+0.72	0.04
Brazil - Nuclebras	2	0.75	380	186	786	50.2	6.56	+0.53	0.06
Canada - Denison	1	0.63	8610	3230	3220	12.7	5970	+0.75	0.05
Canada - Eldorado Uranium District	1	0.67	3260	740	3060	13.3	4280	+0.55	0.05
Canada - Gunnar	1	0.59	2860	1630	17800	2.39	326	+0.98	0.04
Canada - Gunnar (duplicate)	2	0.79	3140	1610	19000	2.13	291	+1.10	0.07
Canada - Key Lakes	2	0.66	69.5	40.2	223	520	1.15	-1.13	0.06
Canada - Macassa	1	0.62	1320	359	14100	2.62	5370	+0.80	0.04
Canada - Madawaska	1	0.59	2700	582	24300	5.74	10200	+0.97	0.05
Canada - Rabbit Lake	2	0.76	338	114	1420	313	0.66	+1.16	0.06
Canada - Rio Algom	1	0.65	8740	2490	8230	28.6	7440	+0.44	0.05
Canada - Stanleigh	1	0.65	595	393	11500	5.78	6850	+0.45	0.05
Canada - Stanrock	1	0.61	2210	1390	3150	13.8	3870	+0.14	0.05
Canada - Stanrock (duplicate)	2	0.61	2210	1390	3150	13.8	3870	+0.15	0.04
Congo - NS	2	0.71	1170	1060	10800	164	31.3	-0.02	0.05
Gabon - Mounana	2	0.80	707	386	2460	632	3.15	+0.46	0.05
Germany - Brunhilde/Menzenschwandt	1	0.63	5700	633	2040	15.3	41.3	+1.50	0.04
Germany - Ellweiler	1	0.67	5230	598	3830	15.8	29.5	+1.39	0.04
Germany - Wismut Mining Area	2	0.69	1300	2300	20100	2000	142	-0.23	0.05
Namibia - Rossing Mine	2	0.93	10.2	170	57.3	123	8.66	+0.08	0.05
Netherlands - Delft	2	0.76	359	477	512	5620	3.92	-0.39	0.05
Romania - Feldioara Mill	1	0.55	3870	1730	21800	57.3	169	+0.74	0.06
Romania - Feldioara Mill (duplicate)	2	0.55	3870	1730	21800	57.3	169	+0.74	0.04
Sweden - Ranstadt	2	0.71	12.2	397	351	204	3.49	+1.68	0.05
USA - Anaconda	1	0.69	2080	339	2430	26.5	30.8	+1.22	0.04
USA - Federal American Partners	2	0.82	61.1	124	914	2540	14.9	+1.96	0.05
USA - Petromic	2	0.82	369	129	1310	39.3	5.17	+0.55	0.05
USA - Shirley Basin	2	0.87	241	12200	331	704	2.3	+1.19	0.05
Yugoslavia - Spisak-Black	2	0.71	530	222	7610	26.7	440	-1.15	0.06
Yugoslavia - Spisak-Yellow	2	0.66	2410	1100	13300	19.4	13.9	+0.85	0.06
Zambia - Mindola Mine	2	0.65	13400	779	39500	1040	708	+0.16	0.05
AngloGold-Ashanti South Uranium Plant									
South Africa - Ore	2	0.0004	31800	9130	12000	1.37	26.4	-0.06	0.05
South Africa - ADU	2	0.75	42	335	172	36.6	3.46	+0.69	0.05
South Africa - U_3O_8	2	0.81	112	268	360	22.1	3.23	+0.70	0.05

[a] Samples were processed in two batches with different methods. See text for details.
[b] Uncertainty is 2×standard error of a single mass spectrometric analysis.

4. Discussion

The Mo isotope composition of UOC samples analyzed in this study span a δ^{98}Mo range of >3‰ from -1.15 to +1.96‰ (Fig. 3; Table 4). The range of δ^{98}Mo observed in the UOC samples is likely related to variable δ^{98}Mo in the parent U ores, Mo isotope fractionation during different UOC production process, and/or industrial contamination of Mo with variable δ^{98}Mo during UOC production. The overall range in δ^{98}Mo observed in the UOC samples is very similar to the

360 δ^{98}Mo range observed in natural materials (Smedley and Kinniburgh, 2017; Kendall et al., 2017).
361 Among the large geological reservoirs of Mo, seawater has the highest δ^{98}Mo with an average
362 value of +2.09 ± 0.10‰ (Greber et al., 2012; Goldberg et al., 2013, Kendall et al., 2017).
363 Removal of Mo from seawater via adsorption onto and/or coprecipitation with ferromanganese
364 sediments results in a ca. 3‰ isotope fractionation with Fe-Mn nodules and crusts typically
365 displaying a δ^{98}Mo value of ca. -1‰ (Barling et al., 2001; Siebert et al., 2003). Similar to
366 seawater, Earth's mantle is relatively homogeneous with respect to its Mo isotope composition
367 but is relatively isotopically light with an average δ^{98}Mo value of -0.21 ± 0.06‰ (Greber et al.,
368 2015). The magnitude of Mo isotope variability observed in molybdenite minerals extracted
369 from crustal rocks spans the entire range of δ^{98}Mo observed in natural materials from ca. -1.62 to
370 +2.27‰ with an average value +0.04 ± 1.04‰ (2σ; Breillat et al., 2016). While the Mo isotope
371 heterogeneity observed in Mo minerals from igneous rocks makes it difficult to estimate the
372 overall Mo isotope composition of the crust, it is likely that much of the δ^{98}Mo variability
373 observed in UOC is inherited from the parent U ores. The observation that UOC contains Mo
374 with essentially a natural isotope composition is important because it demonstrates that industrial
375 processes are unlikely to result in excessive mass-dependent isotope fractionation. Therefore, it
376 is expected that materials from the later stages of the nuclear fuel cycle will contain Mo isotope
377 signatures generated during enrichment and reactor processes that are free from significant
378 isotopic anomalies related to the UOC production process.
379
380 The UOC samples investigated here have an average δ^{98}Mo of +0.55 ± 0.70‰ (1 s.d.) and
381 approximately a normal distribution about the mean (Fig. 3). No strong correlation between
382 δ^{98}Mo and [Mo] is observed. However, we note that UOC samples with elevated Mo/U ratios
383 tend to be isotopically light characterized by the lowest δ^{98}Mo values (Fig. 4), although UOC
384 sample USA – Federal American Partners (δ^{98}Mo = +1.96 ± 0.05‰) clearly diverges from this
385 tendency. The relationships between δ^{98}Mo and Al/U, K/U and Fe/U suggest that UOC samples
386 with the highest levels of matrix elements remaining in the UOC product tend to cluster around
387 δ^{98}Mo values close to the overall average of +0.55‰ (Fig. 4). It is logical that the level of matrix
388 elements remaining in the final UOC product is indicative of how efficiently U was separated
389 from the parent U ore with higher levels of matrix elements associated with less efficient U

separation. Indeed, UOC samples with higher concentrations of Fe typically contain lower U concentrations (Fig. 5). Accordingly, it is plausible that UOC containing high levels of matrix elements also contain Mo derived from the parent U ore that is isotopically unfractionated. If this assumption is true, then it suggests that the average UOC δ^{98}Mo of +0.55 ± 0.70‰ (1SD) is a reasonable estimation of the δ^{98}Mo of the parent U ores and suggests that, on average, U ores contain Mo that is isotopically heavy relative to the bulk continental crust (δ^{98}Mo = 0.04 ± 1.04‰). The most extreme δ^{98}Mo values are associated with UOC samples that contain the least amount of matrix elements (Fig. 4), which is indicative of more efficient separation of U from ore matrix, including Mo. As discussed in more detail below, leaching experiments by Migeon et al. (2018) suggest that UOC production processes that maximize the removal of Mo will generate the largest Mo isotope fractionations between the UOC and parent U ore with the UOC being isotopically heavy relative to the parent U ore. However, we suggest that the relatively normal distribution of δ^{98}Mo values around a mean of +0.55‰ observed in our UOC samples likely indicates that different production processes may lead to either an enrichment of the heavy or the light Mo isotopes in the final UOC product relative to the parent U ore.

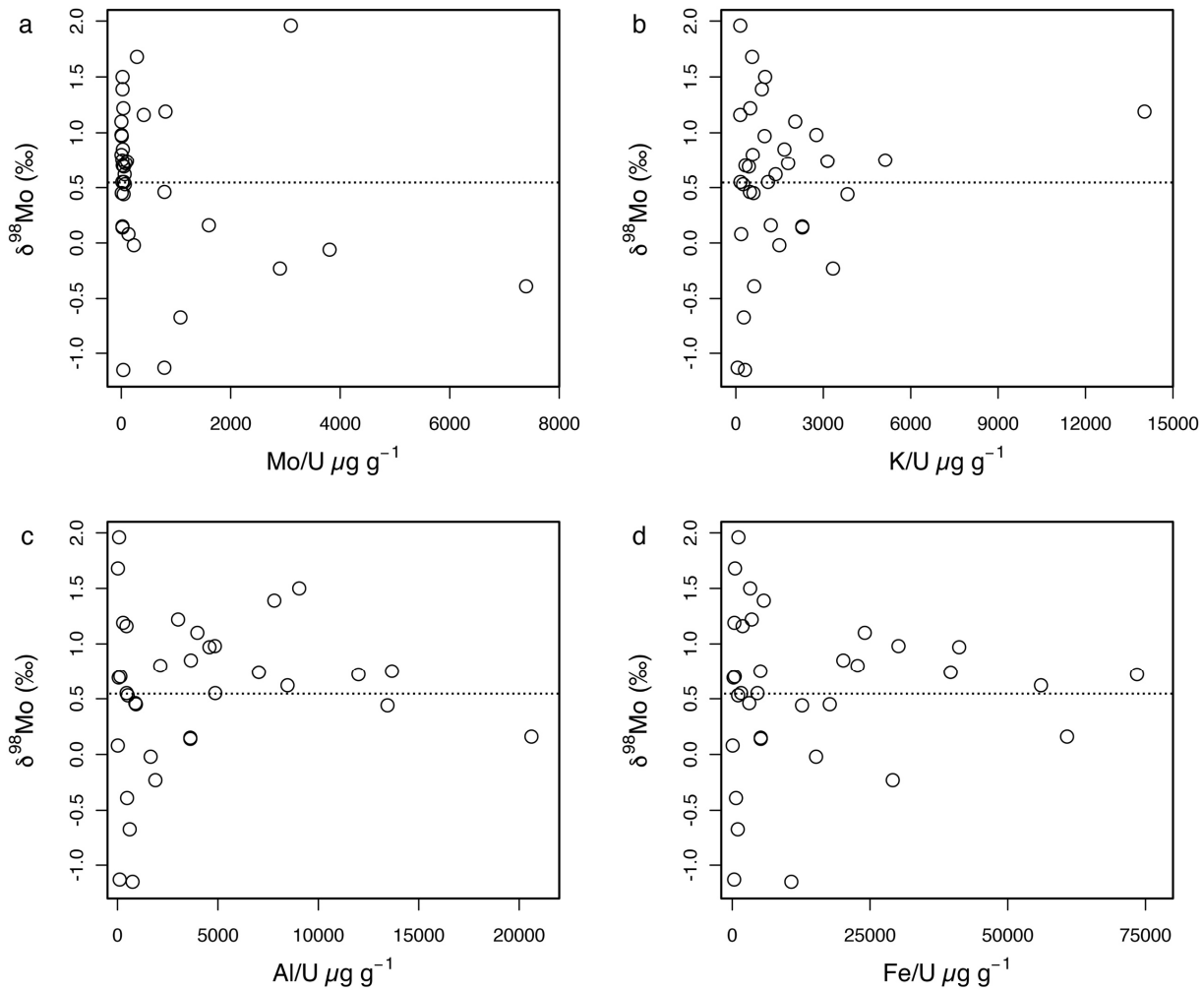

406

407 **Fig. 4.** Plot of δ^{98}Mo versus (a) Mo/U, (b) K/U, (c) Al/U, and (d) Fe/U in UOC samples. The

408 horizontal dashed line is the average δ^{98}Mo of all UOC samples of +0.55‰.

409

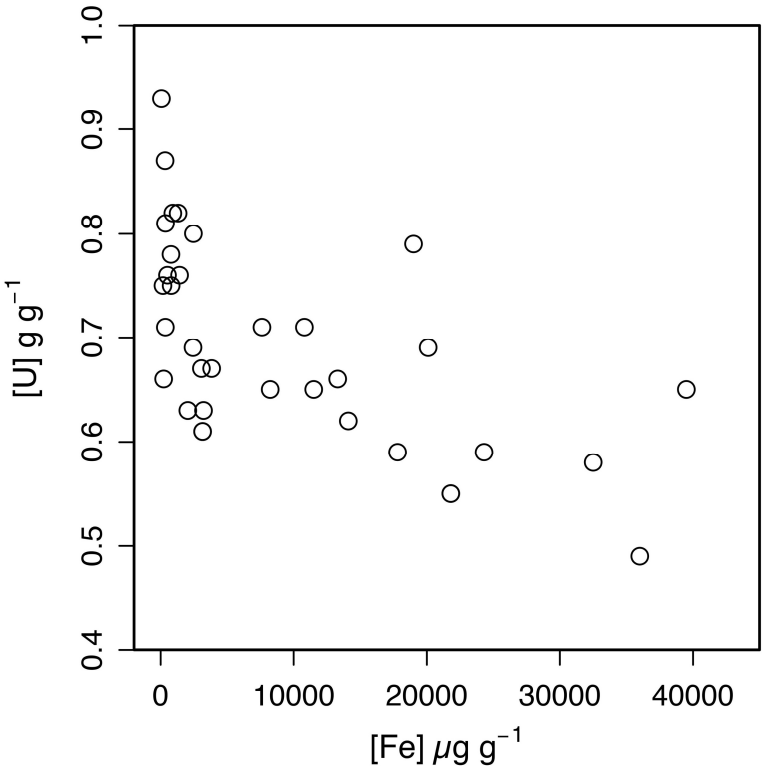

410

411 **Fig. 5.** Plot of Fe concentration versus U concentration in the UOC samples.

412

413 The overall process of chemical weathering of continental igneous rocks results in the
414 preferential transport of heavy Mo isotopes to the ocean (Archer and Vance, 2008; Pearce et al.,
415 2010; Voegelin et al., 2012) which, in addition to sinks that remove isotopically light Mo, lead to
416 the oceans being Earth's most isotopically heavy reservoir of Mo (Kendall et al., 2017). Based
417 on a series of laboratory leaching experiments, Migeon et al. (2018) argue that important
418 chemical weathering processes, such as adsorption and secondary mineral formation, are likely
419 taking place during the leaching of U ores during UOC production, which ultimately results in
420 UOC products containing isotopically heavy Mo relative to the parent U ore. Under acidic
421 leaching conditions with pH between 1 and 2 and in the presence of oxidizing agents HNO_3 or
422 H_2O_2, Migeon et al. (2018) predict that Mo will be efficiently leached from the U ore which
423 should lead to only minor Mo isotope fractionation between UOC and parent U ore and a high
424 yield of Mo through the leaching process. In contrast, acidic leaching procedures that employ
425 MnO_2 or $Fe_2(SO_4)_3$ as oxidizers should promote adsorption of Mo on to secondary minerals
426 leading to a larger Mo isotope fractionation and a lower yield of Mo (Migeon et al., 2018). The

427 samples analyzed from South African AngloGold-Ashanti South Uranium Plant display offset
428 δ^{98}Mo values of ca. +0.75‰ between the ADU (δ^{98}Mo = +0.69 ± 0.05‰) and U_3O_8 (δ^{98}Mo =
429 +0.70 ± 0.05‰) samples relative to the parent U ore (δ^{98}Mo = -0.06 ± 0.05‰; Table 4). It is
430 known that the U ore was leached with sulfuric acid for 18 h at 50-60 °C but it is not known
431 which, if any, oxidizing agents were used (Marks et al., 2015). Based on the observations of
432 Migeon et al. (2018), the Mo isotope data would suggest that adsorption and/or secondary
433 mineral formation occurred during the leaching process thereby leading to the observed δ^{98}Mo
434 offset. Isotope mass balance considerations dictate that leaching conditions that promote
435 significant Mo isotope fractionation will lead to minimized yield of Mo through the leaching
436 process. In the South African samples, the Mo concentration increases from 1.37 μg g^{-1} in the
437 parent U ore to 36.6 μg g^{-1} in the ADU while the other elements such as Al, K, Fe, and Th all
438 strongly decrease (Table 4). The elevated Mo concentration in the ADU product relative to the
439 parent U ore may suggest that the yield of Mo through the leaching process was rather high in
440 contradiction with the prediction from the Mo isotope data, although a more quantitative estimate
441 of the yield is desirable. The possibility of industrial Mo contamination with a δ^{98}Mo of +0.75‰
442 or greater during the UOC production process cannot definitively be ruled out, but the Mo
443 concentration of 36.6 μg g^{-1} in the ADU sample is not anomalously high relative to the suite of
444 UOC samples investigated here. Thus, the Mo isotope fractionation observed between the parent
445 U ore and the ADU and U_3O_8 products agrees reasonably well with the leaching experiments of
446 Migeon et al. (2018).
447
448 Migeon et al. (2018) also specify that UOC production methods employed in the Rössing facility
449 in Namibia are likely to promote large Mo isotope fractionation because MnO_2 and/or $Fe_2(SO_4)_3$
450 are used as oxidants thereby leading to the formation of secondary minerals that can adsorb
451 dissolved Mo and remove it from solution. Under such conditions, it is expected that Mo is
452 efficiently separated from U during UOC production and that the UOC product should have a
453 relatively minor Mo content. A sample of UOC from the Namibia Rössing Mine analyzed in this
454 study has a δ^{98}Mo value of +0.08 ± 0.05‰ and a [Mo] of 123 μg g^{-1} (Table 4). Rather than being
455 significantly isotopically heavy and relatively depleted in Mo, as predicted by Migeon et al.
456 (2018), the UOC sample from the Namibia Rössing Mine is isotopically light and Mo replete
457 relative to the majority of the UOC samples investigated here. Although, it is not possible to

quantify the magnitude of Mo isotope fractionation at the Namibia Rössing Mine with one sample, it is unlikely that this sample experienced significant Mo isotope fractionation unless the parent U ore used was isotopically light. The leaching experiments by Migeon et al. (2018) that used MnO_2 as an oxidizer (i.e. Test#4b) or used no oxidizer (i.e. Test#1a, 1b, and 4a) resulted in the largest Mo isotope fractionations. The δ^{98}Mo values of the final leachates in these experiments were higher by ca. +0.4 to +1.3‰ than the δ^{98}Mo value of the initial U ore. Assuming the UOC from the Namibia Rössing Mine experienced a similar magnitude of Mo isotope fractionation, then the δ^{98}Mo of the parent U ore would need to have been between ca. -1.2 and -0.3‰ which is well within the δ^{98}Mo values observed in molybdenite (Breillat et al., 2016). However, our dataset suggests that the Namibia Rössing Mine UOC contains isotopically light Mo and therefore it is likely unfractionated from Mo contained in its parent U ore.

5. Conclusions

The Mo isotope composition of a geographically diverse suite of UOC samples has been determined by double spike MC-ICP-MS. Amongst all of the samples analyzed, δ^{98}Mo ranged from -1.15 to +1.96‰ with an average of +0.55 ± 0.70‰ (1 s.d.). The δ^{98}Mo range observed in the UOC samples mirrors the range observed in natural materials and demonstrates that UOC production processes do not introduce Mo contamination with a significantly non-natural isotope composition. Therefore, it is expected that Mo entering the nuclear fuel cycle initially contained within UOC and subsequently converted to MoF_6 will have an essentially natural isotope composition, allowing for a more straightforward interpretation of isotopic signatures that are expected to be generated during enrichment and reactor processes.

The variability of δ^{98}Mo observed in UOC reflects the δ^{98}Mo variability in the parent U ores, variable Mo isotope fractionation during UOC production processes, and potentially different sources of Mo contamination with variable δ^{98}Mo. Observations of δ^{98}Mo in molybdenite minerals from crustal rocks span a range larger than that observed in UOC samples, suggesting that much of the δ^{98}Mo variability in UOC can be attributed to δ^{98}Mo variability in the parent U

ores. However, Mo isotope fractionation during UOC production was observed in paired samples of UOC and parent U ore from South Africa with δ^{98}Mo being +0.75‰ higher in the ammonium diuranate (+0.69‰) sample compared to the parent U ore (-0.06‰). The preferential enrichment of heavy Mo isotopes in UOC relative to parent U ores agrees with the observed Mo isotope fractionation during experimental leaching of U ore under leaching conditions representative of industrial processes (Migeon et al., 2018). Thus, both the δ^{98}Mo variability inherent to crustal rocks and minerals and Mo isotope fractionation associated with UOC production contribute to the overall range of δ^{98}Mo observed in UOC samples, while the importance of industrial Mo contamination is still uncertain.

Future research aimed at constraining the Mo isotope composition of U ores would help constrain the sources of δ^{98}Mo variability in UOC, as would analyses of paired samples of UOC and their parent U ores. Ultimately, the Mo isotope composition of UOC will be most useful as a comparative signature to add to the list of parameters used to discriminate between different sources of materials, while the usefulness of Mo isotope signatures produced later in the nuclear fuel cycle are only beginning to be investigated.

Acknowledgements

This work was performed under the auspices of the U.S. Department of Energy by Lawrence Livermore National Laboratory under Contract DE-AC52-07NA27344. Support was provided by the LLNL-LDRD Program under Project No. 18-ERD-016 and the United States Department of Homeland Security's Domestic Nuclear Detection Office through the National Nuclear Forensics Expertise Development Program. The views and conclusions contained in this document are those of the authors and should not be interpreted as representing the official policies, either expressed or implied, of the U.S. Government. LLNL-JRNL-758218

518 **References**
519
520 Archer, C., Vance, D., 2008. The isotopic signature of the global riverine molybdenum flux and
521 anoxia in the ancient oceans. Nature Geoscience, 1: 597.
522 Arnold, G.L., Anbar, A.D., Barling, J., Lyons, T.W., 2004. Molybdenum Isotope Evidence for
523 Widespread Anoxia in Mid-Proterozoic Oceans. Science, 304(5667): 87-90.
524 Barling, J., Arnold, G.L., Anbar, A.D., 2001. Natural mass-dependent variations in the isotopic
525 composition of molybdenum. Earth and Planetary Science Letters, 193(3): 447-457.
526 Breillat, N., Guerrot, C., Marcoux, E., Négrel, P., 2016. A new global database of δ98Mo in
527 molybdenites: A literature review and new data. Journal of Geochemical Exploration,
528 161: 1-15.
529 Brennecka, G.A., Borg, L.E., Hutcheon, I.D., Sharp, M.A., Anbar, A.D., 2010. Natural variations
530 in uranium isotope ratios of uranium ore concentrates: Understanding the 238U/235U
531 fractionation mechanism. Earth and Planetary Science Letters, 291(1): 228-233.
532 Cady, G.H., Hargreaves, G.B., 1961. The vapour pressures of some heavy transition-metal
533 hexafluorides. Journal of the Chemical Society (Resumed), 305(0): 1563-1568.
534 Creech, J.B., Moynier, F., Badullovich, N., 2017. Tin stable isotope analysis of geological
535 materials by double-spike MC-ICPMS. Chemical Geology, 457: 61-67.
536 Dahl, T.W. et al., 2010. The behavior of molybdenum and its isotopes across the chemocline and
537 in the sediments of sulfidic Lake Cadagno, Switzerland. Geochimica et Cosmochimica
538 Acta, 74(1): 144-163.
539 Goldberg, T. et al., 2013. Resolution of inter-laboratory discrepancies in Mo isotope data: an
540 intercalibration. Journal of Analytical Atomic Spectrometry, 28(5): 724-735.
541 Greber, N.D., Puchtel, I.S., Nägler, T.F., Mezger, K., 2015. Komatiites constrain molybdenum
542 isotope composition of the Earth's mantle. Earth and Planetary Science Letters, 421: 129-
543 138.
544 Greber, N.D., Siebert, C., Nägler, T.F., Pettke, T., 2012. δ98/95Mo values and Molybdenum
545 Concentration Data for NIST SRM 610, 612 and 3134: Towards a Common Protocol for
546 Reporting Mo Data. Geostandards and Geoanalytical Research, 36(3): 291-300.
547 IAEA, 1993. Uranium Extraction Technology. Technical Reports Series. INTERNATIONAL
548 ATOMIC ENERGY AGENCY, Vienna.
549 Keegan, E. et al., 2008. The provenance of Australian uranium ore concentrates by elemental and
550 isotopic analysis. Applied Geochemistry, 23(4): 765-777.
551 Kendall, B., Dahl, T.W., Anbar, A.D., 2017. The Stable Isotope Geochemistry of Molybdenum.
552 Reviews in Mineralogy and Geochemistry, 82(1): 683.
553 Krajkó, J., Varga, Z., Yalcintas, E., Wallenius, M., Mayer, K., 2014. Application of neodymium
554 isotope ratio measurements for the origin assessment of uranium ore concentrates.
555 Talanta, 129: 499-504.
556 Kristo, M.J. et al., 2016. Nuclear Forensic Science: Analysis of Nuclear Material Out of
557 Regulatory Control. Annual Review of Earth and Planetary Sciences, 44(1): 555-579.

558 Kristo, M.J., Tumey, S.J., 2013. The state of nuclear forensics. Nuclear Instruments and Methods
559 in Physics Research Section B: Beam Interactions with Materials and Atoms, 294: 656-
560 661.

561 Liang, Y.-H. et al., 2017. Molybdenum isotope fractionation in the mantle. Geochimica et
562 Cosmochimica Acta, 199: 91-111.

563 Marks, N.E. et al., 2015. Technical Report on the Behavior of Trace Elements, Stable Isotopes,
564 and Radiogenic Isotopes During the Processing of Uranium Ore to Uranium Ore
565 Concentrate, Lawrence Livermore National Laboratory, United States.

566 Mayer, A.J., Wieser, M.E., 2014. The absolute isotopic composition and atomic weight of
567 molybdenum in SRM 3134 using an isotopic double-spike. Journal of Analytical Atomic
568 Spectrometry, 29(1): 85-94.

569 McManus, J., Nägler, T.F., Siebert, C., Wheat, C.G., Hammond, D.E., 2002. Oceanic
570 molybdenum isotope fractionation: Diagenesis and hydrothermal ridge-flank alteration.
571 Geochemistry, Geophysics, Geosystems, 3(12): 1-9.

572 Migeon, V., Bourdon, B., Pili, E., Fitoussi, C., 2015. An enhanced method for molybdenum
573 separation and isotopic determination in uranium-rich materials and geological samples.
574 Journal of Analytical Atomic Spectrometry, 30(9): 1988-1996.

575 Migeon, V., Bourdon, B., Pili, E., Fitoussi, C., 2018. Molybdenum isotope fractionation during
576 acid leaching of a granitic uranium ore. Geochimica et Cosmochimica Acta, 231: 30-49.

577 Nägler, T.F., Siebert, C., Lüschen, H., Böttcher, M.E., 2005. Sedimentary Mo isotope record
578 across the Holocene fresh–brackish water transition of the Black Sea. Chemical Geology,
579 219(1): 283-295.

580 Neubert, N., Nägler, T.F., Böttcher, M.E., 2008. Sulfidity controls molybdenum isotope
581 fractionation into euxinic sediments: Evidence from the modern Black Sea. Geology,
582 36(10): 775.

583 Pearce, C.R., Burton, K.W., von Strandmann, P.A.E.P., James, R.H., Gíslason, S.R., 2010.
584 Molybdenum isotope behaviour accompanying weathering and riverine transport in a
585 basaltic terrain. Earth and Planetary Science Letters, 295(1): 104-114.

586 Rudge, J.F., Reynolds, B.C., Bourdon, B., 2009. The double spike toolbox. Chemical Geology,
587 265(3): 420-431.

588 Siebert, C., Nägler, T.F., Kramers, J.D., 2001. Determination of molybdenum isotope
589 fractionation by double-spike multicollector inductively coupled plasma mass
590 spectrometry. Geochemistry, Geophysics, Geosystems, 2(7).

591 Siebert, C., Nägler, T.F., von Blanckenburg, F., Kramers, J.D., 2003. Molybdenum isotope
592 records as a potential new proxy for paleoceanography. Earth and Planetary Science
593 Letters, 211(1): 159-171.

594 Skierszkan, E.K., Amini, M., Weis, D., 2015. A practical guide for the design and
595 implementation of the double-spike technique for precise determination of molybdenum
596 isotope compositions of environmental samples. Analytical and Bioanalytical Chemistry,
597 407(7): 1925-1935.

598 Smedley, P.L., Kinniburgh, D.G., 2017. Molybdenum in natural waters: A review of occurrence,
599 distributions and controls. Applied Geochemistry, 84: 387-432.

600 Švedkauskaitė-LeGore, J., Rasmussen, G., Abousahl, S., Belle, P.v., 2008. Investigation of the
601 sample characteristics needed for the determination of the origin of uranium-bearing
602 materials. Journal of Radioanalytical and Nuclear Chemistry, 278(1): 201-209.

603 Varga, Z. et al., 2017. Identification of uranium signatures relevant for nuclear safeguards and
604 forensics. Journal of Radioanalytical and Nuclear Chemistry, 312(3): 639-654.

605 Varga, Z., Wallenius, M., Mayer, K., Keegan, E., Millet, S., 2009. Application of Lead and
606 Strontium Isotope Ratio Measurements for the Origin Assessment of Uranium Ore
607 Concentrates. Analytical Chemistry, 81(20): 8327-8334.

608 Voegelin, A.R. et al., 2012. The impact of igneous bedrock weathering on the Mo isotopic
609 composition of stream waters: Natural samples and laboratory experiments. Geochimica
610 et Cosmochimica Acta, 86: 150-165.

611 Wedepohl, H.K., 1995. The composition of the continental crust. Geochimica et Cosmochimica
612 Acta, 59(7): 1217-1232.